

## RECONFIGURABLE FILTER ANTENNAS FOR PULSE ADAPTATION IN UWB COGNITIVE RADIO SYSTEMS

M. Al-Husseini<sup>1,\*</sup>, L. Safatly<sup>1</sup>, A. Ramadan<sup>1</sup>, A. El-Hajj<sup>1</sup>, K. Y. Kabalan<sup>1</sup>, and C. G. Christodoulou<sup>2</sup>

<sup>1</sup>Department of Electrical and Computer Engineering, American University of Beirut, P. O. Box 11-0236, Beirut 1107 2020, Lebanon

<sup>2</sup>Department of Electrical and Computer Engineering, University of New Mexico, Albuquerque, NM 87131, USA

**Abstract**—The design of filter antennas with reconfigurable band stops is proposed. They are meant for employment in ultrawideband cognitive radio (UWB-CR) systems, where unlicensed users communicate using adaptive pulses that have nulls in the bands used by licensed users. Neural networks or circuits implementing the Parks-McClellan algorithm can generate such pulses. With filter antennas, reconfigurable bandstop filters are first designed, to induce adaptive nulls in UWB pulses, and are then integrated in the feed line of a UWB antenna. The advantages of this combination are discussed. The filters are based on split-ring resonators (SRRs) and complementary split-ring resonators (CSRRs). The relationship between the SRR and CSRR parameters and the stop band is also studied.

### 1. INTRODUCTION

With the demand on radio spectrum increasing, Cognitive Radio (CR) [1] is thought of as a solution to the spectrum scarcity problem and is expected revolutionize the way it is allocated. The current spectrum allocation regulations assign specific bands to particular services, and grant licensed band access to licensed users only. In a CR network following the hierarchical access model [2], the intelligent radio part allows unlicensed users (secondary users) to access spectrum bands licensed to primary users, while avoiding interference with them. In this model, two approaches to spectrum sharing between primary

---

*Received 18 November 2011, Accepted 23 December 2011, Scheduled 4 January 2012*

\* Corresponding author: Mohammed Al-Husseini (husseini@ieee.org).

and secondary users have been considered: spectrum underlay and spectrum overlay.

In the underlay approach, secondary users should operate below the noise floor of primary users, and thus severe constraints are imposed on their transmission power (should be less than  $-42$  dBm/MHz). One way to achieve this is to spread the transmitted signals of secondary users over an ultra-wide frequency band, leading to a short-range high-data-rate transmission with extremely low power. The spectrum overlay (also termed opportunistic spectrum access or OSA) approach imposes restrictions on when and where secondary users may transmit rather on their transmission power. In this approach, secondary users avoid higher priority users through the use of spectrum sensing and adaptive allocation. They identify and exploit the spectrum holes defined in space, time, and frequency. The underlay and overlay approaches can be employed simultaneously for further spectrum efficiency improvement.

Ultrawideband (UWB) communication, on the other hand, is commonly carried out by transmitting extremely short pulses. As per FCC regulations, UWB systems are allowed to operate in the 3.1–10.6 GHz band without a license requirement, but under very strict transmission power limits. This property of UWB, in addition to its other advantages, makes it suitable as the enabling technology for underlay Cognitive Radio [3].

Though usually associated with the underlay mode, UWB can also be used in the overlay Cognitive Radio mode. In this mode, the transmitted power can be increased to a level that is comparable to that of licensed systems (an advantage would be long-

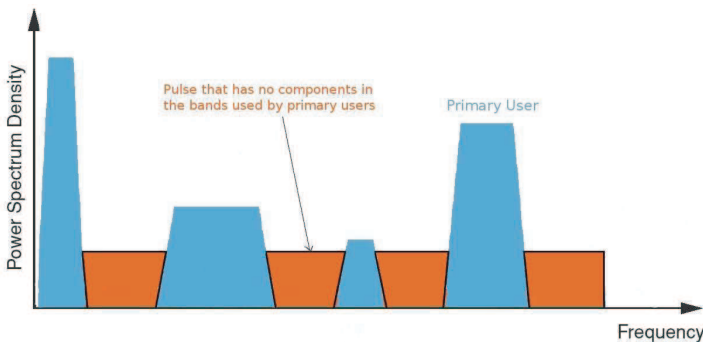


**Figure 1.** Overlay UWB cognitive radio: the UWB pulse has nulls in the bands used by primary users and its power is comparable to that of a primary service.

distance communication as compared to short- and medium-range communication in the underlay case), but this requires the UWB transmitter to avoid spectrum bands that are used by other systems. This can be achieved by the use of adaptive UWB pulses characterized by the ability to form, in their spectral masks, nulls in the bands used by existing narrow-band wireless services [4]. This is illustrated in Fig. 1.

The design of adaptive UWB pulses is at the core of this paper. In Section 2, the use of neural networks and the Parks-McClellan algorithm for UWB pulse adaptation is discussed through examples. The design of a reconfigurable bandstop filter is presented in Section 3. This filter can be used to create adaptive nulls in a UWB pulse, at specific frequencies, before transmitting the pulse using a UWB antenna. The antenna and the reconfigurable bandstop filter are then combined in Section 4, by integrating the filter on the antenna's feed line, to form a reconfigurable filter antenna. The Parks-McClellan algorithm and neural networks can generate UWB pulses with deep nulls in the desired bands, but they are hard to implement in hardware and have increased time requirements. The proposed reconfigurable bandpass filter is much easier to implement, although it does not offer the same deep nulls. Other advantages of the filter antenna design are indicated in Sections 3 and 4.

## 2. SIGNAL PROCESSING TECHNIQUES

The Parks-McClellan algorithm [5, 6] is an iterative algorithm utilized for the design of efficient finite impulse response (FIR) filters with linear phase. It obtains the optimum Chebyshev approximation on separate intervals corresponding to passbands and/or stopbands. Adaptive pulses that satisfy the FCC spectral mask and avoid interference to multiple narrowband services within the spectral range can be generated using this Parks-McClellan algorithm [7].

As an example, we consider two narrowband services that could be operated in the 3.5 and 5.5 GHz bands (WiMAX and WLAN bands). Four cases are treated: Case 1 when both services are not active in a certain time interval, Case 2 when only the 3.5 GHz system is operating, Case 3 when only the 5.5 GHz service is operating, and Case 4 when both are active. The power spectral density (PSD) plots of the pulses generated using the Parks-McClellan algorithm for the four cases are shown in Fig. 2. The plots demonstrate that the generated pulses well satisfy the FCC spectral mask, and that a null is created at the desired frequency band depending on the case taken.

Neural networks can also be used to produce FCC-compliant UWB

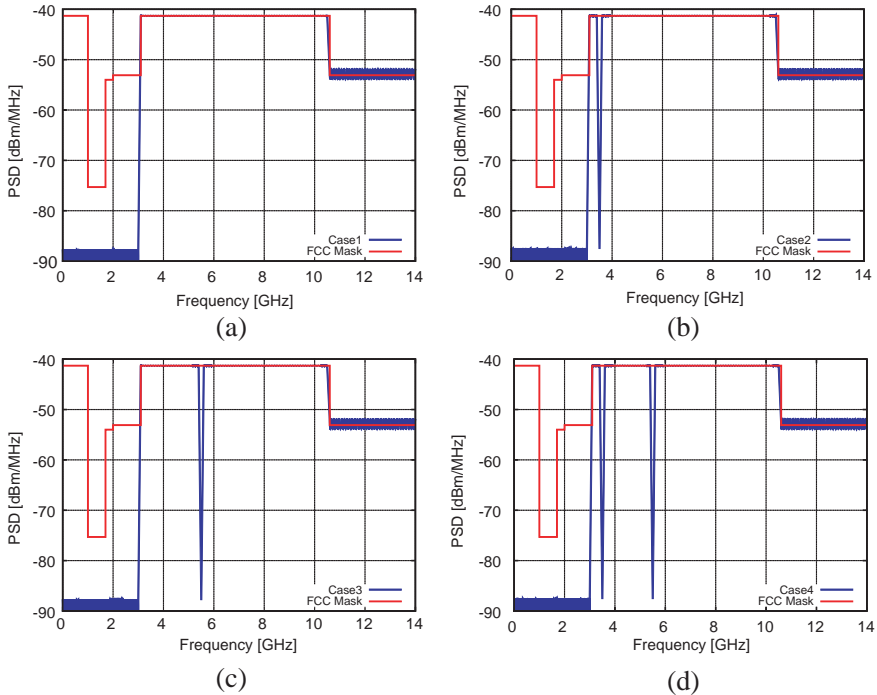


**Figure 2.** Adaptive pulses using Parks-McClellan with possible nulls at 3.5 and 5.5 GHz. (a) Case 1: no nulls. (b) Case 2: null at 3.5 GHz. (c) Case 3: null at 5.5 GHz. (d) Case 4: null at 3.5 and 5.5 GHz.

pulses with adaptive nulls. Neural networks are composed of simple elements operating in parallel, which are inspired by biological nervous systems [8]. As in nature, the network function is determined by the connections between the elements. A neural network is trained to perform a particular function by adjusting the values of the connections (weights) between elements until the output due to a particular input matches the target. For each of the four cases in the previous example, a radial basis function (RBF) network [9] with the Gaussian function [10] as its basis waveform is trained. The output pulse PSD plots are shown in Fig. 3.

### 3. BANDSTOP FILTER DESIGN

Both the Parks-McClellan algorithm and neural networks are robust in their generation of UWB pulses that satisfy the FCC spectral mask and show nulls in desired bands. However, they have their limitations, especially their complicated hardware implementation and

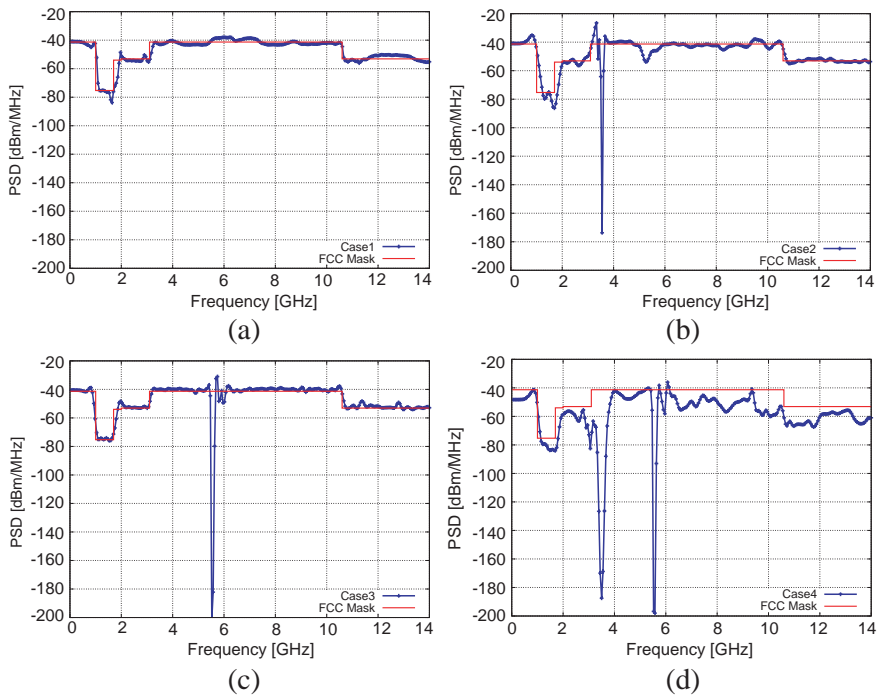


**Figure 3.** Adaptive pulses using neural networks with possible nulls at 3.5 and 5.5 GHz. (a) Case 1: no nulls. (b) Case 2: null at 3.5 GHz. (c) Case 3: null at 5.5 GHz. (d) Case 4: null at 3.5 and 5.5 GHz.

the time requirement to achieve their goal pulses. Besides, with Parks-McClellan algorithm, it is not possible to independently specify all of the desired parameters [5].

A different approach to inducing adaptive nulls in a UWB pulse is through the use of reconfigurable bandstop (notch) RF filters. A pulse, originally conforming to the FCC mask, is sent through such a filter. As a result, nulls are created in the pulse in the bands where the filter possesses notches. A UWB pulse that can be used for such purpose is given by [11]

$$\nu(t) = \sin [2\pi f_0 (t - t_0)] \exp \left[ -\frac{(t - t_0)^2}{2\tau^2} \right] \quad (1)$$

where  $f_0 = 6$  GHz,  $\tau = 80$  ps, and  $t_0 = 5\tau$ .

In this section, a design method for reconfigurable bandstop filters is discussed. A notch filter can be obtained by integrating a complementary split-ring resonator (CSRR) in a  $50 \Omega$  microstrip line,

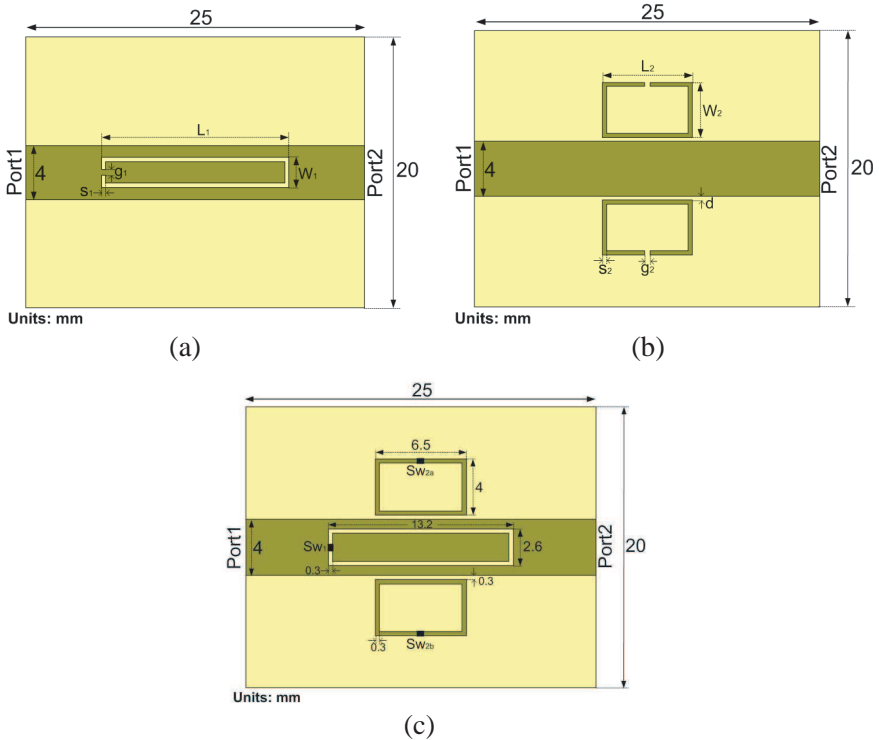


**Figure 4.** Two bandstop filters and a combined reconfigurable version. (a) Filter 1: CSRR is etched on a  $50\ \Omega$  microstrip line. (b) Filter 2: a pair of identical SRRs are placed next to a  $50\ \Omega$  microstrip line. (c) Reconfigurable filter: the CSRR and SRRs are combined and switches are used for reconfigurability.

as shown in Fig. 4(a), or by placing split-ring resonators (SRRs) in proximity of the microstrip line, as in Fig. 4(b). SRRs, originally proposed in [12], have been of great interest for the design of negative permeability and left-handed (LH) materials. CSRRs, which are proposed in [13], are the dual counterparts of SRRs, and are used for the synthesis of negative-permittivity media. An RF signal fed to one port of the filter is rejected in a frequency range where permittivity and/or permeability are negative. This frequency range depends on the SRR or CSRR size and other characteristics. It is a well known property that increasing the size of the SRR or the CSRR will decrease the frequency at which the notch appears. The other characteristics will be studied below. The filters in Fig. 4 are printed on a 1.52 mm-thick Rogers RO3203 substrate with  $\epsilon_r = 3.02$ . The microstrip line is

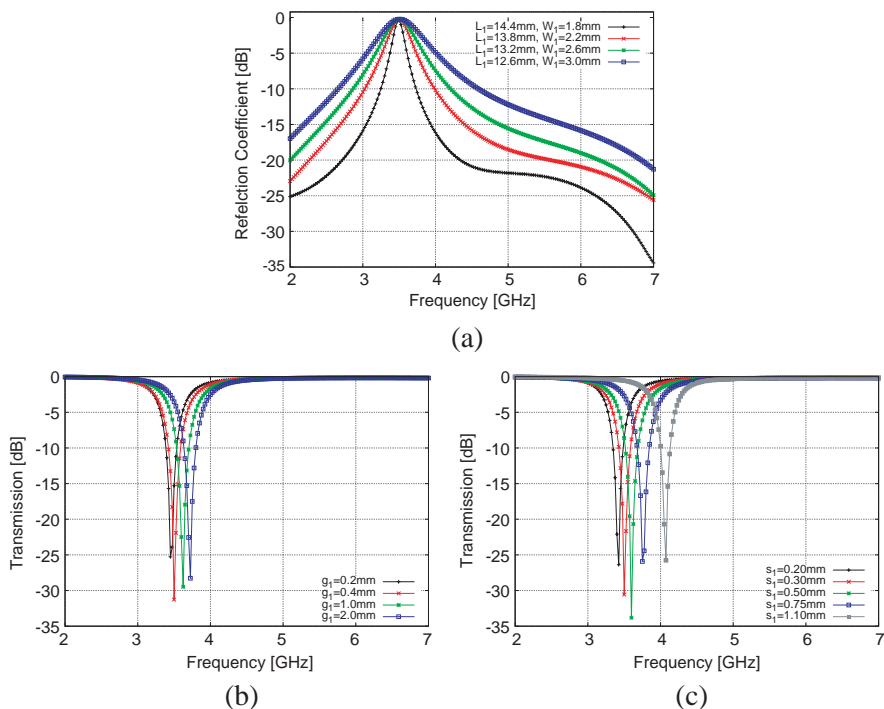


**Figure 5.** Effects of changing the CSRR dimensions. (a) Changing  $L_1$  and  $W_1$  ( $g_1 = 0.4\text{ mm}$  and  $s_1 = 0.3\text{ mm}$ ). (b) Changing  $g_1$  ( $L_1 = 13.2\text{ mm}$ ,  $W_1 = 2.6\text{ mm}$ , and  $s_1 = 0.3\text{ mm}$ ). (c) Changing  $s_1$  ( $L_1 = 13.2\text{ mm}$ ,  $W_1 = 2.6\text{ mm}$ , and  $g_1 = 0.4\text{ mm}$ ).

4 mm in width.

The CSRR in Fig. 4(a) is designed so that the band notch is centered at 3.5 GHz. Fixing  $g_1$  at 0.4 mm and  $s_1$  at 0.3 mm, the effect of changing  $L_1$  and  $W_1$  on the reflection coefficient  $S_{11}$  is shown in Fig. 5(a). As the ratio  $L_1/W_1$  decreases, the notch becomes wider. Setting  $L_1 = 13.2\text{ mm}$ ,  $W_1 = 2.6\text{ mm}$ , and  $s_1 = 0.3\text{ mm}$ , the increase in  $g_1$  will increase the notch frequency, as shown by the  $S_{21}$  plots of Fig. 5(b). Increasing  $s_1$  also increases the notch frequency, as appears in Fig. 5(c).

The two SRRs in Fig. 4(b) are identical and are placed symmetrically around the microstrip line. The use of such identical SRRs helps to strengthen the notch ( $S_{11}$  value is closer to 0 dB) and keeps the symmetry of the design. The SRRs are designed for a notch frequency of 5.5 GHz. Referring to Fig. 6, the following conclusions can be made: decreasing  $L_2/W_2$  decreases the notch width (opposite

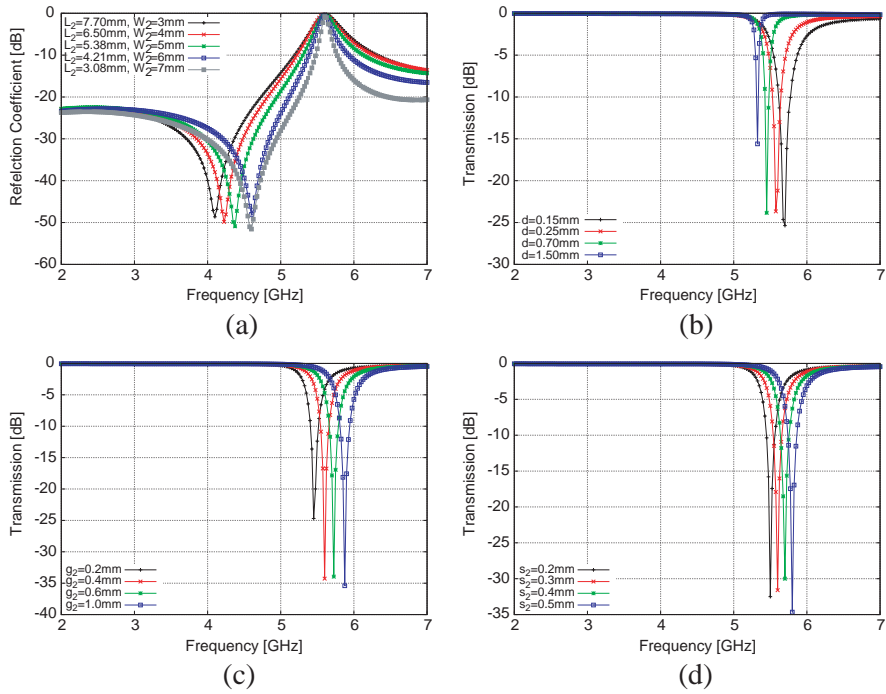


**Figure 6.** Effects of changing the SRR dimensions. (a) Changing  $L_2$  and  $W_2$  ( $d = s_2 = 0.3\text{ mm}$  and  $g_2 = 0.4\text{ mm}$ ). (b) Changing  $d$  ( $L_2 = 6.5\text{ mm}$ ,  $W_2 = 4\text{ mm}$ ,  $s_2 = 0.3\text{ mm}$  and  $g_2 = 0.4\text{ mm}$ ). (c) Changing  $g_2$  ( $L_2 = 6.5\text{ mm}$ ,  $W_2 = 4\text{ mm}$  and  $d = s_2 = 0.3\text{ mm}$ ). (d) Changing  $s_2$  ( $L_2 = 6.5\text{ mm}$ ,  $W_2 = 4\text{ mm}$ ,  $d = 0.3\text{ mm}$  and  $g_2 = 0.4\text{ mm}$ ).

to the CSRR case), increasing  $d$  decreases the notch frequency (the notch becomes weaker and eventually disappears for large  $d$  values), and increasing  $g_2$  or  $s_2$  increases the notch frequency (similar to the CSRR case).

A notch caused by an SRR can be turned on and off by placing an RF switch over the SRR's gap, and one caused by a CSRR can also be switched on and off using a switch mounted across the CSRR's slot. As a result, a reconfigurable bandstop filter can be designed using SRRs and CSRRs that are controlled via RF switches. In a similar example to the one in Section 2, a filter with the ability to selectively have a band notches at 3.5 and 5.5 GHz is designed and is shown in Fig. 4(c). Three RF switches are used, with two of them operated in parallel. The switching cases and the corresponding switch states are listed in Table 1.



**Table 1.** Switch states for the different cases.

Case	$Sw_1$	$Sw_{2a}$ & $Sw_{2b}$
1	OFF	ON
2	ON	ON
3	OFF	OFF
4	ON	OFF

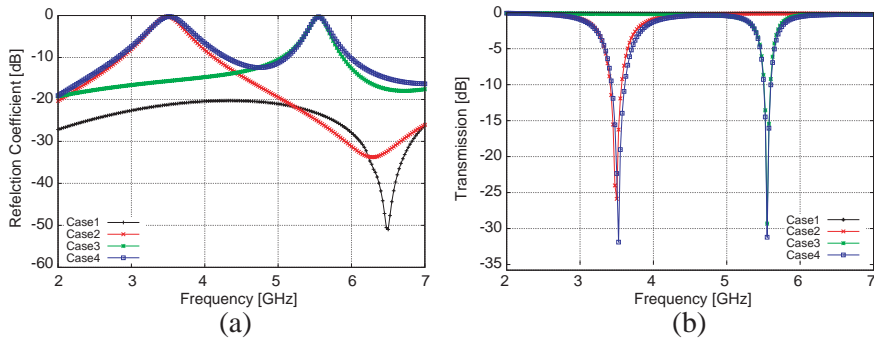


**Figure 7.**  $S_{11}$  and  $S_{21}$  of the reconfigurable filter. (a)  $S_{11}$  of reconfigurable filter. (b)  $S_{21}$  of reconfigurable filter.

The reflection  $S_{11}$  and transmission  $S_{21}$  of the reconfigurable filter are plotted in Fig. 7. As expected, Case 1 results in no band stops, Case 2 in a notch at 3.5 GHz, Case 3 in a notch at 5.5 GHz, and finally Case 4 in the two band stops together.

The results in Figs. 5, 6, 7 are computed in Ansoft HFSS [14]. To validate these results, the same reconfigurable filter is simulated in Agilent ADS [15]. The  $S_{21}$  plots for the four switching cases are given in Fig. 8. A complete match is attained.

Some notes are worth mentioning here. The first is that the presented filter designs employ single-ring SRRs and CSRRs. Single-ring SRRs and CSRRs are simpler in structure and thus have less parameters to care about when used in design. Another advantage is that only one RF switch is needed per single-ring SRR or CSRR as opposed to two when dual-ring SRRs and CSRRs are used. A second remark is that more SRRs and CSRRs can be implemented in the filter as needed. This has to do with the number of narrowband primary services to which interference should be avoided. A third note is that CSRRs do not have to be implemented in the microstrip line. They can be integrated in the ground plane below, thus giving more space for several of them, if more nulls are to be created in the pulse. Last,

a number of notches can be realized using only SRRs, or only CSRRs.

To assess the applicability of the reconfigurable filter in UWB pulse adaptation, the pulse in Equation (1) is used as the input to Port 1 of the filter. The PSD plots of the output pulse for the four

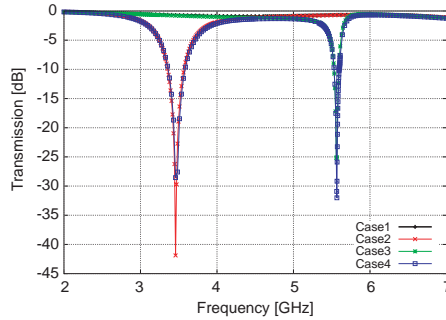


**Figure 8.**  $S_{21}$  of the reconfigurable filter computed in ADS.

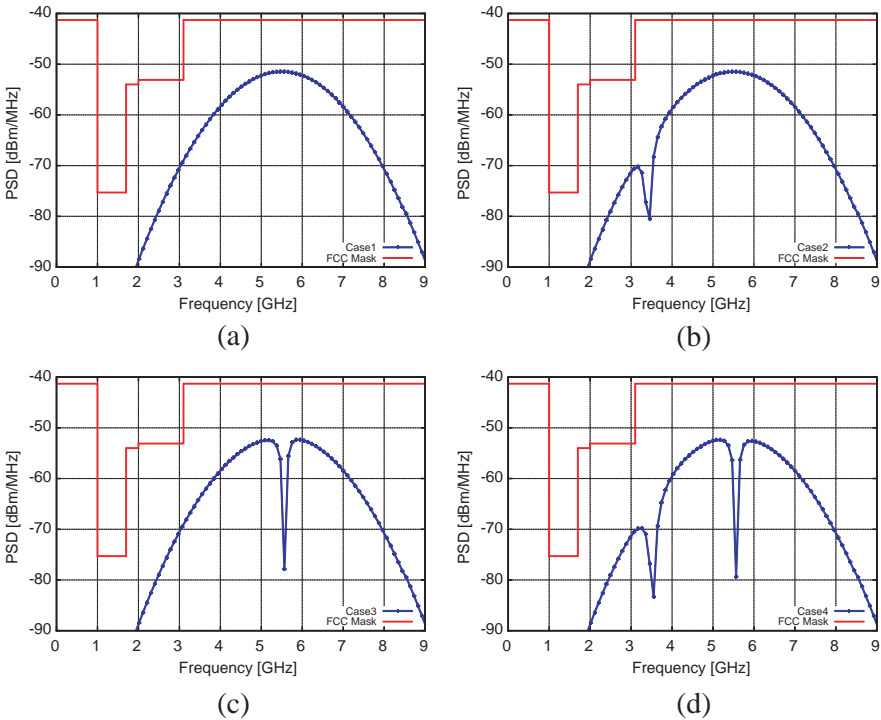


**Figure 9.** Gaussian-modulated sinusoidal pulse with possible nulls at 3.5 and 5.5 GHz. (a) Case 1: no nulls. (b) Case 2: null at 3.5 GHz. (c) Case 3: null at 5.5 GHz. (d) Case 4: null at 3.5 and 5.5 GHz.

switching cases are depicted in Fig. 9. The plots show the appearance of nulls at the desired frequencies. These nulls are not as deep as in the neural network case, but they are still quite satisfactory given the simplicity of the filter structure and the fast switching speed, which is the speed of the RF switches used. Implementing the filter with an adequate number of notches is possible by including the necessary combinations of SRRs and CSRRs. The presence of the adaptive nulls allows to raise the pulse power without causing interference to the primary users.

#### 4. FILTER ANTENNA DESIGN

A UWB pulse with adaptive nulls is transmitted using a UWB antenna. In this Section, a design that integrates the reconfigurable bandstop filter with a UWB antenna is presented. The filter of Fig. 4(c) is embedded in the feed line of a UWB microstrip antenna to form the system in Fig. 10. The UWB antenna is based on a rounded patch and a partial rectangular ground plane. The Rogers RO3203 material is used for the 1.52 mm-thick substrate. The SRRs and CSRR have the same dimensions as in Fig. 4(c). A prototype of this filter antenna is fabricated and the reflection coefficient is measured. A photograph

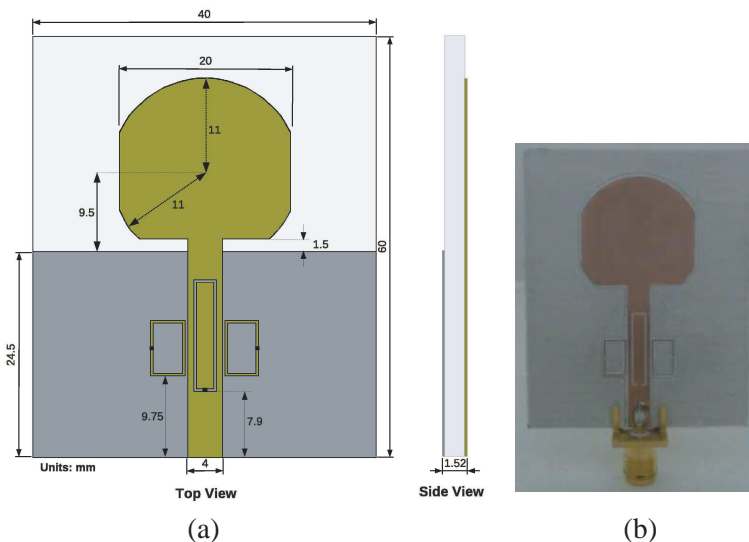


**Figure 10.** Filter antenna: reconfigurable bandstop filter in Fig. 4(c) integrated in the feed line of the antenna. (a) Antenna configuration. (b) Prototype photo.

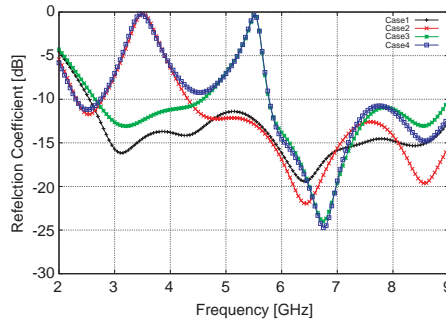


**Figure 11.** Simulated reflection coefficient. Case 1: no notches. Case 2: notch at 3.5 GHz. Case 3: notch at 5.5 GHz. Case 4: notches at 3.5 and 5.5 GHz.

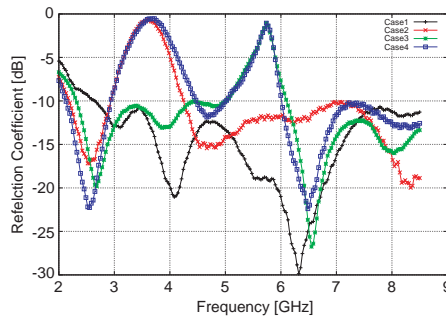


**Figure 12.** Measured reflection coefficient. Case 1: no notches. Case 2: notch in 3.5 GHz band. Case 3: notch in 5.5 GHz band. Case 4: notches in 3.5 and 5.5 GHz bands.

of the prototype is shown in Fig. 10(b). The simulated and measured  $S_{11}$  plots are shown in Figs. 11 and 12, respectively. Good analogy is witnessed. The slight increase in the notch frequencies is attributed to inaccuracies in the fabrication process resulting in smaller substrate thickness in etched areas. This effect could be countered by slightly increasing the sizes of the CSRR and the SRR pair. Case 1, where no band notches exist, allows the antenna to sense the UWB range to determine the narrowband primary services that are transmitting inside the range. In the other three cases, the notches block the transmission of pulse components in the 3.5 GHz band, the 5.5 GHz band, or both. In the receiving case, this filter antenna can receive the adaptive pulse without the signal of the primary service.

The normalized gain patterns of the filter antenna, for some

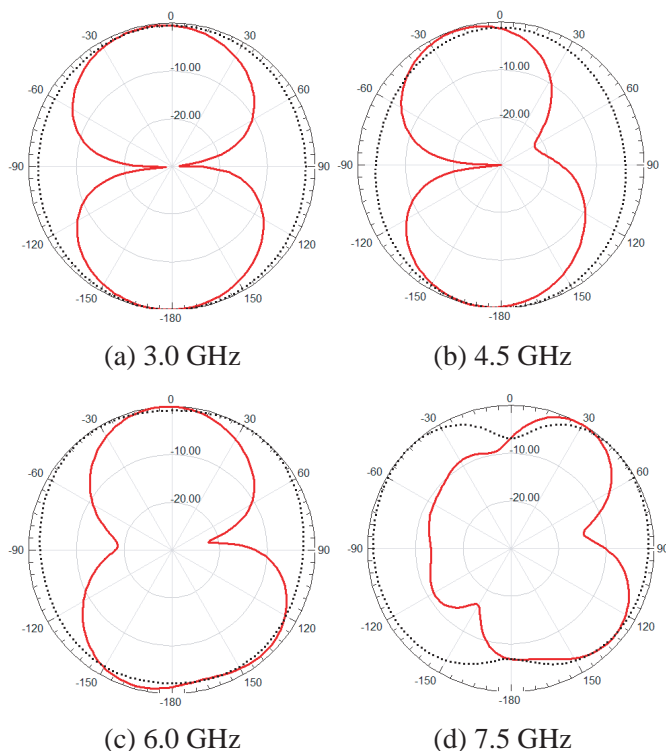


**Figure 13.** Normalized gain patterns in the  $H$ -plane (dotted line) and  $E$ -plane (solid line). Antenna has omnidirectional patterns.

frequencies, are shown in Fig. 13. The antenna has good omnidirectional patterns, and this is expected since the antenna is a printed monopole with a small ground plane not covering the radiating patch. The realized peak gain of the antenna is plotted in Fig. 14 for Case 1 and Case 4. In Case 4, the gain drops sharply, to below  $-10$  dB, at 3.5 GHz (band where permittivity is negative) and at 5.5 GHz (band where permeability is negative). In these two bands, very high reflections occur at the antenna’s input.

The advantages of the reconfigurable bandstop filter, discussed in Section 3, are inherited by this filter antenna. SRRs and CSRRs have previously been used to design antennas with band notches. However, in most cases, the band notches are fixed, once the antenna is fabricated, and are always present in its frequency profile, as in [16] and [17]. Reconfigurable band notches are discussed in [18], where CSRRs are etched on the patch and electronic switches mounted across. The location of the switches on the patch makes it hard to design

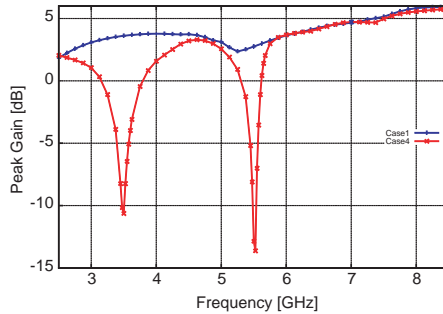


**Figure 14.** Realized peak gain of the antenna. Case 1: gain is positive. Case 4: gain is negative in the 3.5 and 5.5 GHz bands.

and connect their DC biasing network. More recently, a design with a tunable band notch has been reported in [19]. Herein, the band rejection is narrowband and limited to the 5.2–5.7 GHz. The authors did not disclose any information on having notches in other bands. For the filter antenna presented in this paper, the band notches are reconfigurable, and the switches are integrated away from the radiating parts, so they could be DC-biased with little effects on the antenna characteristics. On the other hand, the design is easily expandable, meaning that rejection of more bands is possible by adding extra SRRs or CSRRs (to the feed line or ground) with the appropriate dimensions to obtain the desired notch frequency and width.

It is of interest to compare this design to the one in [20], which is based on a reconfigurable bandpass filter. Both antennas can be operated in full UWB mode for channel sensing. However, the passband filter in [20] results in narrowband operation, which is used for communication over a white space in overlay cognitive radio. A bandstop filter, on the opposite, leads to a narrowband rejection, which is needed when UWB-CR is used in an overlay mode, with adaptive UWB pulses transmitted at high power levels. A final note is that filter antennas, such as the one presented here, can also be used in underlay CR for they can operate as UWB. Their ability to dynamically reject a band is an advantage, even when the transmitted UWB pulses satisfy the FCC power limits. In this case, more unlicensed users can operate, without increasing the noise floor of primary users.

## 5. CONCLUSION

Pulse adaptation for application in UWB-CR was discussed in this paper. The Parks-McClellan algorithm and neural networks can generate robust pulses with adaptive nulls that prevent interference

to primary users, however they are slow and difficult to implement in hardware.

A design method for reconfigurable bandstop filters was presented. These filters can adaptively introduce nulls in UWB pulses, are simple in design, and can be directly integrated with UWB antennas. Although the nulls they produce are not as deep as those generated by neural networks, these nulls can still limit interference to licensed narrowband services and allow unlicensed users to increase their output power to achieve communication over longer distances.

## REFERENCES

1. Mitola, J. and G. Q. Maguire, "Cognitive radio: Making software radios more personal," *IEEE Pers. Commun.*, Vol. 6, No. 4, 13–18, Aug. 1999.
2. Chen, K.-C. and R. Prasad, *Cognitive Radio Networks*, John Wiley & Sons, West Sussex, United Kingdom, 2009.
3. Arslan, H. and M. Sahin, "UWB-based cognitive radio networks," *Cognitive Wireless Communication Networks*, Springer, USA, 2007.
4. Zhang, H., X. Zhou and T. Chen, "Ultra-wideband cognitive radio for dynamic spectrum accessing networks," *Cognitive Radio Networks*, CRC Press, Boca Raton, Florida, 2009.
5. Parks, T. and J. McClellan, "Chebyshev approximation for nonrecursive digital filters with linear phase," *IEEE Transactions on Circuit Theory*, Vol. 19, No. 2, 189–194, Mar. 1972.
6. McClellan, J. and T. Parks, "A personal history of the Parks-McClellan algorithm," *IEEE Signal Processing Magazine*, Vol. 22, No. 2, 82–86, Mar. 2005.
7. Shi, X., "Adaptive UWB pulse design method for multiple narrowband interference suppression," *The 2010 IEEE International Conference on Intelligent Computing and Intelligent Systems (ICIS 2010)*, 545–548, Missouri, USA, 2010.
8. Hopfield, J. J., "Neural networks and physical systems with emergent collective computational abilities," *Proceedings of the National Academy of Sciences*, Vol. 79, 2554–2558, Washington DC, USA, 1982.
9. Powell, J. D., "Radial basis function approximations to polynomials," *Numerical Analysis 1987*, 223–241, Dundee, UK, 1987.
10. Bin, L., Z. Zheng, and Z. Weixia, "A novel spectrum adaptive UWB pulse: Application in cognitive radio," *The 2009 IEEE*

- Vehicular Technology Conference*, 1–5, Anchorage, AK, USA, 2009.
11. Kanj, H. and M. Popovic, “Microwave-range broadband Dark Eyes antenna: Detailed analysis and design,” *IEEE Antennas and Wireless Propagation Letters*, Vol. 4, 262–265, 2005.
  12. Pendry, J. B., A. J. Holden, D. J. Robbins, and W. J. Stewart, “Magnetism from conductors and enhanced nonlinear phenomena,” *IEEE Trans. Microw. Theory Tech.*, Vol. 47, No. 11, 2075–2084, 1999.
  13. Falcone, F., T. Lopetegui, M. A. G. Laso, J. D. Baena, J. Bonache, M. Beruete, R. Marques, F. Martn, and M. Sorolla, “Babinet principle applied to the design of metasurfaces and metamaterials,” *Physical Review Letters*, Vol. 93, No. 19, 197401–1–197401-4, Nov. 2004.
  14. Ansoft HFSS, Pittsburg, PA 15219, USA.
  15. Agilent ADS, Santa Clara, CA 95051, USA.
  16. Li, C.-M. and L.-H. Ye, “Improved dual band-notched UWB slot antenna with controllable notched bandwidths,” *Progress In Electromagnetics Research*, Vol. 115, 477–493, 2011.
  17. Liao, X.-J., H.-C. Yang, N. Han, and Y. Li, “Aperture UWB antenna with triple band-notched characteristics,” *Electronics Letters*, Vol. 47, No. 2, 77–79, Jan. 2011.
  18. Al-Husseini, M., A. Ramadan, A. El-Hajj, K. Y. Kabalan, Y. Tawk, and C. G. Christodoulou, “Design based on complementary split-ring resonators of an antenna with controllable band notches for UWB cognitive radio applications,” *The 2011 IEEE International Symposium on Antennas and Propagation (APS/URSI 2011)*, 1120–1122, Spokane, WA, USA, Jul. 3–8, 2011.
  19. Gardner, P., P. S. Hall, M. R. Hamid, and F. Ghanem, “Reconfigurable antennas for cognitive radio,” *The 2011 IEEE-APS Topical Conference on Antennas and Propagation in Wireless Communications (APWC 2011)*, 1225–1228, Torino, Italy, Sept. 12–16, 2011.
  20. Al-Husseini, M., A. Ramadan, M. E. Zamudio, C. G. Christodoulou, A. El-Hajj, and K. Y. Kabalan, “A UWB antenna combined with a reconfigurable bandpass filter for cognitive radio applications,” *The 2011 IEEE-APS Topical Conference on Antennas and Propagation in Wireless Communications (APWC 2011)*, 902–904, Torino, Italy, Sept. 12–16, 2011.